9th ANKARA INTERNATIONAL AEROSPACE CONFERENCE **AIAC-2017-089**
20-22 September 2017 - METU, Ankara TURKEY

# MULTI BLOCK AND PARALLEL COMPUTATIONS OF ROTOR FAN USING THREE DIMENSIONAL EULER EQUATIONS

Emre Özmen[1]
Middle East Technical University
Ankara, TURKEY

Sinan Eyi[2]
Middle East Technical University
Ankara, TURKEY

## ABSTRACT

*The aim of this study is to develop an efficient fan/compressor rotor analysis tool using Newton-GMRES method. Three dimensional Euler equations are solved for transonic compressor rotor. Solution method is a matrix free solution technique hence it is not required the Jacobian matrix evaluation and flow equations are solved implicitly. Governing equations are casted into rotational coordinate system to make the problem available to use implicit solver. Computational domain is divided into optimum number of blocks and each block is solved by different processor using parallel computing. NASA Rotor 67 transonic fan is analyzed by solver and solutions are compared with the experimental test results of NASA.*

## INTRODUCTION

Researchers intend to solve a problem as accurate as and as fast as possible using computational fluid dynamics. Generally these two requests affect each other oppositely. Definition of a problem and chosing the effective solution method is the most important starting point for simulation. Considiring these situations, it will be a major mistake to expect a solution of unsteady problem from an implicit solver. Turbomachinery flow field is very complex and it includes wide range of time and length scales. This kind of flow can be named as highly unsteady and also the cost of the solution is very expensive [Adamcyzk, 1984]. Althought turbomachinery problems need to unsteady solutions, flow field can be viewed or presented as steady state with casting equations into rotating coordinate system which is also can be called as non-inertial reference of frame [Ghosh, 1996]. It is provided by attaching the coordinate system to the blade. The success of casting equations in cylindrical rotating coordinate system for turbine blade was encouraged the researchers for different applications [Adamcyzk, Celestina, Beach and Barnett, 1990]. Axial compressor rotor was solved in rotating cartesian coordinate sytem [Chima, 1990] and it is effieciency was compared with fixed reference frame [Ghosh, 1996]. Method is widely using in rotational systems flow field analysis for example helicopter rotors [Agarwal and Deese, 1987; Srinivasan, Baeder, Obayashi and McCroskey, 1992] and turbomahinery applications [Holmes and Tong, 1985; Weber, Thoe and Delaney, 1989; Arnone, 1994]. Two important factors in coordinate tranformation are coriolis and centrifugal forces and their

[1] Graduate Student in Aerospace Engineering, Email: e199440@metu.edu.tr
[2] Associate Professor in Aerospace Engineering, Email: seyi@metu.edu.tr

implementations. The details of the coordinate transform, effects of transforming on governing equations and residual vector is presented in chapter Method.

Recent advances in computer technology and solution algorithms allow efficient solution of very large linear systems of equations. These advances have been motivating researchers to develop implicit algorithms to solve the flow equations since usage of implicit methods is more benefical compared to explicit ones. Implicit flow solvers are more stable and the residual can be reduced to very low values within a small number of iterations. In addition, the equations of different disciplines can be strongly coupled with flow equations in an implicit algorithm. Characterized by large variation in Mach number and unsteadiness turbomachinery flows are special flow types in which physical and numerical modeling is difficult. In such flow conditions, due to the numerical stiffness of the system, convergences problems may be observed. Implicit methods may have more advantages to avoid these problems. Providing quadratic convergence, Newton method is one of the preferred algorithms to solve non-linear equations. The requirement for the evaluation and the solution of large Jacobian matrix is the main disadvantage of Newton method. The Jacobian matrix is evaluated by taking the derivatives of residual vector with respect to flow variable vector. Although the size of this matrix can be very large, it is sparse in the most of the flow problems. The selection of good initial solution is important in Newton method. If the initial solution is not chosen properly, Newton method may diverge. To keep the advantages and to avoid disadvantages of Newton method, in recent years, Jacobian-free Newton methods are getting more attention. One of these methods is Newton-GMRES method. Newton-GMRES method has been developed and applied in different areas of CFD. Some of these physics models [Knoll and Keyes, 2004]. A Newton-Krylov method can be summarized as an iterative method which is a combination of a linear iterative method. GMRES is used for solving linear systems which is a Krylov subspace method [Saad and Schultz, 1986]. In this study, Newton-GMRES method is used for turbomachinery flow analysis. A cell centered finite volume code is developed by using the three dimensional Euler equations. The fluxes are computed using [Leer, 1982] upwind scheme. Flow equations are solved implicitly by Newton-GMRES method and the boundary conditions are implemented implicitly.

## METHOD

### Governing Equations

Three dimensional unsteady Euler equations in fixed Cartesian coordinate system can be written as follows:

$$\frac{\partial q}{\partial t}+\frac{\partial f}{\partial x}+\frac{\partial g}{\partial y}+\frac{\partial h}{\partial z}=0 \tag{1}$$

where

$$q=\begin{bmatrix}\rho \\ \rho u_a \\ \rho v_a \\ \rho w_a \\ \rho e\end{bmatrix} \quad f=\begin{bmatrix}\rho u_a \\ \rho u_a^2+p \\ \rho u_a v_a \\ \rho u_a w_a \\ \rho u_a h\end{bmatrix} \quad g=\begin{bmatrix}\rho v_a \\ \rho v_a u_a \\ \rho v_a^2+p \\ \rho v_a w_a \\ \rho v_a h\end{bmatrix} \quad h=\begin{bmatrix}\rho w_a \\ \rho w_a u_a \\ \rho w_a v_a \\ \rho w_a^2+p \\ \rho w_a h\end{bmatrix} \tag{2}$$

Total energy can be defined as:

$$e=\frac{p}{\rho(\gamma-1)}+\frac{1}{2}\left(u_a^2+v_a^2+w_a^2\right) \tag{3}$$

$$h = e + \frac{p}{\rho} \tag{4}$$

Right hand side of equation (1) is equal to zero. Velocity components $(u, v, w)$ in flux vectors are absolute velocities so they denoted by subscript $a$ in stationary Cartesian coordinate system. These leads that residual vector only includes the flux residuals with absolute velocities. Converting the coordinate system from inertial to non-inertial disturbs the residual vector strictly in momentum equations which is named as source term. Velocities in flux vectors include the relative velocities with related in rotational direction. Equations (5) shows the three dimensional Euler equations in Cartesian $(x, y, z)$ coordinate system which is rotating with constant angular $\Omega$ velocity about the $x$ - axis [Weber et al. 1989].

$$\frac{\partial q}{\partial t} + \frac{\partial f}{\partial x} + \frac{\partial g}{\partial y} + \frac{\partial h}{\partial z} = s \tag{5}$$

where

$$q = \begin{bmatrix} \rho \\ \rho u_r \\ \rho v_r \\ \rho w_r \\ \rho e \end{bmatrix} \quad f = \begin{bmatrix} \rho u_r \\ \rho u_r^2 + p \\ \rho u_r v_r \\ \rho u_r w_r \\ \rho u_r h \end{bmatrix} \quad g = \begin{bmatrix} \rho v_r \\ \rho v_r u_r \\ \rho v_r^2 + p \\ \rho v_r w_r \\ \rho v_r h \end{bmatrix} \quad h = \begin{bmatrix} \rho w_r \\ \rho w_r u_r \\ \rho w_r v_r \\ \rho w_r^2 + p \\ \rho w_r h \end{bmatrix} \quad s = \begin{bmatrix} 0 \\ 0 \\ \rho\Omega^2 y - 2\rho\Omega w_r \\ \rho\Omega^2 z + 2\rho\Omega v_r \\ 0 \end{bmatrix} \tag{6}$$

In equation (6), momentum equations in directions $y, z$ are affected from Centrifugal and Coriolis forces. Velocities in flux vectors are described with subscript $r$ which is refer to relative velocity components.

The Cartesian equations are mapped to generalized $(\xi, \eta, \zeta)$ coordinate system using standard methods and resulting equations are as follows:

$$\frac{\partial Q}{\partial \tau} + \frac{\partial F}{\partial \xi} + \frac{\partial G}{\partial \eta} + \frac{\partial H}{\partial \zeta} = S \tag{7}$$

problem is solved as resulting steady-state form:

$$\frac{\partial F}{\partial \xi} + \frac{\partial G}{\partial \eta} + \frac{\partial H}{\partial \zeta} = S \tag{8}$$

where

$$F = \frac{1}{J}\begin{bmatrix} \rho U' \\ \rho u_a U' + \xi_x p \\ \rho v_a U' + \xi_y p \\ \rho w_a U' + \xi_z p \\ \rho e U' + pU \end{bmatrix} \quad G = \frac{1}{J}\begin{bmatrix} \rho V' \\ \rho u_a V' + \eta_x p \\ \rho v_a V' + \eta_y p \\ \rho w_a V' + \eta_z p \\ \rho e V' + pV \end{bmatrix} \quad H = \frac{1}{J}\begin{bmatrix} \rho W' \\ \rho u_a W' + \zeta_x p \\ \rho v_a W' + \zeta_y p \\ \rho w_a W' + \zeta_z p \\ \rho e W' + pW \end{bmatrix} \quad S = \frac{1}{J}\begin{bmatrix} 0 \\ 0 \\ -\rho w_a \Omega \\ \rho v_a \Omega \\ 0 \end{bmatrix} \tag{9}$$

In equation (9) $U,V,W$ and $U^{'},V^{'},W^{'}$ represent absolute and relative contravariant velocity components respectively [Chima, 1990]

$$\begin{aligned} U &= \xi_x u_a + \xi_y v_a + \xi_z w_a \qquad & U^{'} &= \xi_x u_r + \xi_y v_r + \xi_z w_r \\ V &= \eta_x u_a + \eta_y v_a + \eta_z w_a \qquad & V^{'} &= \eta_x u_r + \eta_y v_r + \eta_z w_r \\ W &= \zeta_x u_a + \zeta_y v_a + \zeta_z w_a \qquad & W^{'} &= \zeta_x u_r + \zeta_y v_r + \zeta_z w_r \end{aligned} \tag{10}$$

where

$$\begin{aligned} u_r &= u_a \\ v_r &= v_a - \Omega z \\ w_r &= w_a + \Omega y \end{aligned} \tag{11}$$

and metric terms are given by the equations:

$$\begin{aligned} \xi_x &= J\left(y_\eta z_\zeta - y_\zeta z_\eta\right) \quad & \xi_y &= J\left(x_\zeta z_\eta - x_\eta z_\zeta\right) \quad & \xi_z &= J\left(x_\eta y_\zeta - x_\zeta y_\eta\right) \\ \eta_x &= J\left(y_\zeta z_\xi - y_\xi z_\zeta\right) \quad & \eta_y &= J\left(x_\xi z_\zeta - x_\zeta z_\xi\right) \quad & \eta_z &= J\left(x_\zeta y_\xi - x_\xi y_\zeta\right) \\ \zeta_x &= J\left(y_\xi z_\eta - y_\eta z_\xi\right) \quad & \zeta_y &= J\left(x_\eta z_\xi - x_\xi z_\eta\right) \quad & \zeta_z &= J\left(x_\xi y_\eta - x_\eta y_\xi\right) \end{aligned} \tag{12}$$

The inverse of Jacobian of the transformation is defined as

$$\frac{1}{J} = \begin{vmatrix} x_\xi & x_\eta & x_\zeta \\ y_\xi & y_\eta & y_\zeta \\ z_\xi & z_\eta & z_\zeta \end{vmatrix} \tag{13}$$

**Spatial Discretization**

A cell centered finite volume method can be written as a flux balance across a cell:

$$S_{i,j,k} = F_{i+\frac{1}{2},j,k} - F_{i-\frac{1}{2},j,k} + G_{i,j+\frac{1}{2},k} - G_{i,j-\frac{1}{2},k} + H_{i,j,k+\frac{1}{2}} - H_{i,j,k-\frac{1}{2}} \tag{14}$$

where $i,j,k$ index denote the cell center location and $i \pm 1/2, j \pm 1/2, k \pm 1/2$ corresponds to the cell inter face location. The fluxes are discretized by upwind scheme and method of van Leer [Leer, 1982] is used for flux vector splitting. Discretization scheme can be written as:

$$\begin{aligned} S_{i,j,k} = &\left[F^+\left(Q_L\right) + F^-\left(Q_R\right)\right]_{i+\frac{1}{2},j,k} - \left[F^+\left(Q_L\right) + F^-\left(Q_R\right)\right]_{i-\frac{1}{2},j,k} \\ &+ \left[G^+\left(Q_L\right) + G^-\left(Q_R\right)\right]_{i,j+\frac{1}{2},k} - \left[G^+\left(Q_L\right) + G^-\left(Q_R\right)\right]_{i,j-\frac{1}{2},k} \\ &+ \left[H^+\left(Q_L\right) + H^-\left(Q_R\right)\right]_{i,j,k+\frac{1}{2}} - \left[H^+\left(Q_L\right) + H^-\left(Q_R\right)\right]_{i,j,k-\frac{1}{2}} \end{aligned} \tag{15}$$

where $F^{\pm}, G^{\pm}, H^{\pm}$ are called as splitted flux vectors. They are calculated using van Leer flux vector splitting method. $Q_{L,R}$ are left and right state flow variable vectors. Flow variables are calculated at the cell center so they are not stated at cell interface. They are interpolated from cell center to cell interface as follows:

$$\begin{aligned}(Q_L)_{i+\frac{1}{2}} &= (Q)_i \\ (Q_R)_{i+\frac{1}{2}} &= (Q)_{i+1}\end{aligned} \tag{16}$$

Second order accuracy in upwind discretization is obtained using MUSCL (Monotonic Upstream Centered Scheme Conservation Law) [Leer, 1979].

$$\begin{aligned}(Q_L)_{i+\frac{1}{2}} &= Q_i + \frac{1}{4}\left\{\phi(r)\left[(1-\kappa)\nabla + (1+\kappa)\Delta\right]\right\}_i \\ (Q_R)_{i+\frac{1}{2}} &= Q_{i+1} - \frac{1}{4}\left\{\phi(r)\left[(1-\kappa)\Delta + (1+\kappa)\nabla\right]\right\}_{i+1}\end{aligned} \tag{17}$$

where

$$\begin{aligned}\Delta_i &\equiv Q_{i+1} - Q_i \\ \nabla_i &\equiv Q_i - Q_{i-1}\end{aligned} \tag{18}$$

Higher order scheme is used to solve discontinuities (for example shock waves) with high accuracy. Sudden changing of flow variables between two neighbor cells, create numerical oscillations in the solution. In equation (17), $\phi(r)$ is the limiter function. Limiter functions should use to prevent oscillations in higher order schemes such as MUSCL. A limiter in MUSCL is used to reduce the scheme to one-sided in the shock region and oscillations are removed [Yıldırım, 2017]. Equation (17) can be rearranged using Van Albada Limiter as follows [Anderson, Thomas and Leer, 1986]:

$$\begin{aligned}(Q_L)_{i+\frac{1}{2}} &= Q_i + \left\{\frac{s}{4}\left[(1-\kappa s)\nabla + (1+\kappa s)\Delta\right]\right\}_i \\ (Q_R)_{i+\frac{1}{2}} &= Q_{i+1} - \left\{\frac{s}{4}\left[(1-\kappa s)\Delta + (1+\kappa s)\nabla\right]\right\}_{i+1}\end{aligned} \tag{19}$$

where

$$s = \frac{2\Delta\nabla + \varepsilon}{\Delta^2 + \nabla^2 + \varepsilon} \tag{20}$$

and $\varepsilon$ is chosen as a small number such as $1\times10^{-6}$ for preventing division by zero. Lastly, in equation (19), chosen of $(\kappa = -1)$ is corresponds to second order fully upwind differencing and $(\kappa = 1/3)$ to third order upwind biased differencing.

**Boundary Conditions**

Boundary conditions are another significant part of flow solvers. Implementing of proper type is essential to achieve accurate results. Types of boundary conditions are varied by flow problem. Turbomachinery flows are generally include inflow, outflow, wall and periodic boundary conditions.

In rotating coordinate system solutions, flow variables are calculated from absolute velocities and fluxes are calculated from relative velocities. At inlet of transonic compressors, absolute velocity lie as subsonic but relative velocity passes from subsonic to supersonic while from hub to shroud due to increasing of radius. In this work, transonic fan is used as test case so subsonic inflow is chosen for absolute velocity which is called in literature as subsonic inflow with specified total conditions (total condition preserved boundary condition) [Chen, 1991].

Total temperature, total pressure and flow angles is specified [Chima, 1990]. For subsonic case, four information (total temperature, total pressure, $v$ and $w$ velocities) are specified from outside the domain and one (upstream Riemann invariant) is extrapolated from the interior of the computational domain. Only upstream running Riemann invariant $R^-$ is used in this type boundary condition. The Riemann invariant is calculated using absolute velocities. $R^-$ and normalized contravariant velocity ($\bar{U}$) can be written with general notation as follows:

$$R^- = \bar{U} - \frac{2a}{\gamma - 1} \tag{21}$$

where

$$\bar{U} = \frac{\xi_x}{|\nabla\xi|}u + \frac{\xi_y}{|\nabla\xi|}v + \frac{\xi_z}{|\nabla\xi|}w \tag{22}$$

and

$$|\nabla\xi| = \sqrt{\xi_x^2 + \xi_y^2 + \xi_z^2} \tag{23}$$

In this work, flow is perpendicular at inlet and there is only one component of velocity. Inlet face of computational domain is also perpendicular and there is only one component of metrics. Equation (21) is rewritten as [Chen, 1991]:

$$R^- = u_i - \frac{2a_i}{\gamma - 1} = u_b - \frac{2a_b}{\gamma - 1} \tag{24}$$

In equation (24), Riemann invariant is extrapolated from interior to boundary. Specified conditions are written using isentropic relations as follows:

$$p_b = p_o\left[1 + \frac{\gamma - 1}{2}M_b^2\right]^{-\left(\frac{\gamma}{\gamma-1}\right)} \tag{25}$$

$$T_b = T_o\left[1 + \frac{\gamma - 1}{2}M_b^2\right]^{-1} \tag{26}$$

where $p_o$ is the specified total pressure and $T_o$ is the specified total temperature. The remained velocity components are also specified from outside the domain as equal to zero.

$$\begin{aligned} v_b &= 0 \\ w_b &= 0 \end{aligned} \tag{27}$$

Mach number at the boundary can be calculated using the Rieman invariant and the boundary velocity which is the solution of the quadratic equation [Chima, 1990] in equation (28).

$$u_b = \frac{(\gamma - 1)R^- + \sqrt{2(1-\gamma)\left(R^-\right)^2 + 4(\gamma + 1)C_pT_0}}{\gamma + 1} \tag{28}$$

At the outlet, subsonic outflow boundary condition is implemented. Static pressure is specified from the outside of the computational domain as back pressure. Density and three velocities are extrapolated from the interior cells.
For the solid walls (hub case, shroud case and blade), inviscid wall boundary condition is used for Euler equations. Wall boundary conditions are calculated at cell faces and fluxes use relative velocity therefore rotational velocity is added externally for inviscid wall boundary condition equations. Solution of Navier-Stokes equations is not required relative velocity modification due to zero velocity at viscous wall boundary condition.
Turbomachinery problems are periodic flows. Characteristic of periodicity allows that solution does not require the fully flow domain. Generally, one passage between neighbor two blades is chosen as computational domain and periodic boundary condition is applied to starting and ending faces of periodicity. In this work, one blade flow domain is solved similar as literature works and periodic boundary type is implemented to provide periodicity.
One-to-one blocking boundary conditions is used for between the two blocks in contacted with the same cell faces. At the matched faces, ghost cell variables are equalized the interior cell variables of neighbor block. In case of parallel computing while all blocks are solved by different processor, processors have to communicate each other and they have to send and receive variable information to the neighbors.

**Flow Solver**

Flow equations are solved implicitly by Newton-GMRES method. Newton method solves the system of nonlinear equations. Resulting of Newton method, the problem is converted to solution of linear system of equations. Linear systems can be solved directly or iteratively. UMFPACK [Davis, 2003] and PARDISO [Schenk and Gartner, 2004] are two of the well-known direct solvers in academic area. High computational cost of direct solution is made iterative solvers more popular in last years and GMRES [Saad, 1986] is one of them which is categorized in Krylov subspace method. However, iterative solution of linear system is cheaper than direct solution, storage and solution of flow Jacobian is still expensive. Flow Jacobian matrix is occurred at the end of each exact solution of Newton iteration. Newton-GMRES method overcomes from the cost flow Jacobian problem as using inexact solution of Newton method. Control the iteration number of Newton equations save the time as observable and keep the accuracy in reasonable level. As a result of Newton-GMRES method convergence is accelerated. The stopping criteria of Newton iteration is written as:

$$\left\| \hat{R}(\hat{Q}_k) + \hat{R}'(\hat{Q}_k)\Delta\hat{Q}_k \right\|_2 \le \eta_k \left\| \hat{R}(\hat{Q}_k) \right\|_2 \tag{29}$$

where $\eta_k$ is control the accuracy of iterative solution while choosing $\left[0,1\right)$ and $\hat{Q}_k$ is the step size.

$$R'(\hat{Q})v \approx \frac{R(\hat{Q}+\varepsilon v) - R(\hat{Q})}{\varepsilon} \tag{30}$$

While using Newton-GMRES method, there is no need to compute Jacobian matrix which is one of the most important feature of this method. It only requires the action of the Jacobian $\hat{R}'\left(\hat{Q}_k\right)$ on a vector $v$ which can be approximated by finite difference and this process leads us to make computation without evaluating a matrix which means the process is matrix free [Knoll and Keyes, 2004]. Perturbation magnitude $\varepsilon$ is chosen as $4\times10^{-8}$ for optimum perturbation in Euler equations [Onur and Eyi, 2005]. Algorithm of Newton-GMRES can present as follows:

1) Initial guess for solution $\left(x_k^0\right)$
2) Initial guess for Newton update $\left(s_k^0\right)$
3) Selecting stopping criteria of Newton iteration $\left(\eta_k\right)$
4) $r_k^0 = F^{'}\left(x_k\right)s_k^0 - F\left(x_k\right)$
5) $\beta_k = \left\| r_k^0 \right\|_2$
6) $v_1 = r_k^0 / \beta_k$
7) While $\left\| r_k^0 \right\|_2 \geq \eta_k \left\| F\left(x_k\right) \right\|_2$ do
8) $m = m+1$
9) $Av_m = F^{'}\left(x_k\right)v_m; \quad w_m = Av_m$
10) Create Upper-Hessenberg matrix $h_{i,m} = \left(w_m^T, v_i\right), \quad \forall i = 1,2,...,m$
11) Orthogonalization $\hat{v}_{m+1} = w_m - \sum_{i=1}^{m} h_{i,m} v_i$
12) $h_{m+1,m} = \left\| \hat{v}_{m+1} \right\|_2$
13) $J\left(y_m\right) = \min \left\| \beta_k e_1 - \bar{H}_m y_m \right\|_2$ where $e_1 = \left[1,...,0\right]_{m+1}$, $y_m = \left[\ \right]_m$, $\bar{H}_m \left[\ \right]_{(m+1)\times m}$
14) Update solution $x_k = x_0 + V_m y_m$ where $V_m = \left[v_1, v_2, ..., v_m\right]_{m\times m}$

## RESULTS

**Test Case**

NASA Rotor 67 is transonic axial flow fan rotor which was designed and tested at the NASA Glenn center. It has 22 blades which are rotating 16043 rpm in the designed condition. The inlet relative Mach number is 1.38 at the rotor tip and tip speed is equal to 428.9 m/s. Tip radius is 25.7 cm at the leading edge and 24.25 cm at trailing edge. There is 1 mm tip clearance along the tip. The design pressure ratio is 1.63 at 33.25 kg/s mass flow rate. Geometry and flow conditions at inlet and outlet for near peak efficiency and for near stall conditions are presented in details at NASA report [Strazisar, 1989]. Computational results are compared with experimental results for both running conditions.

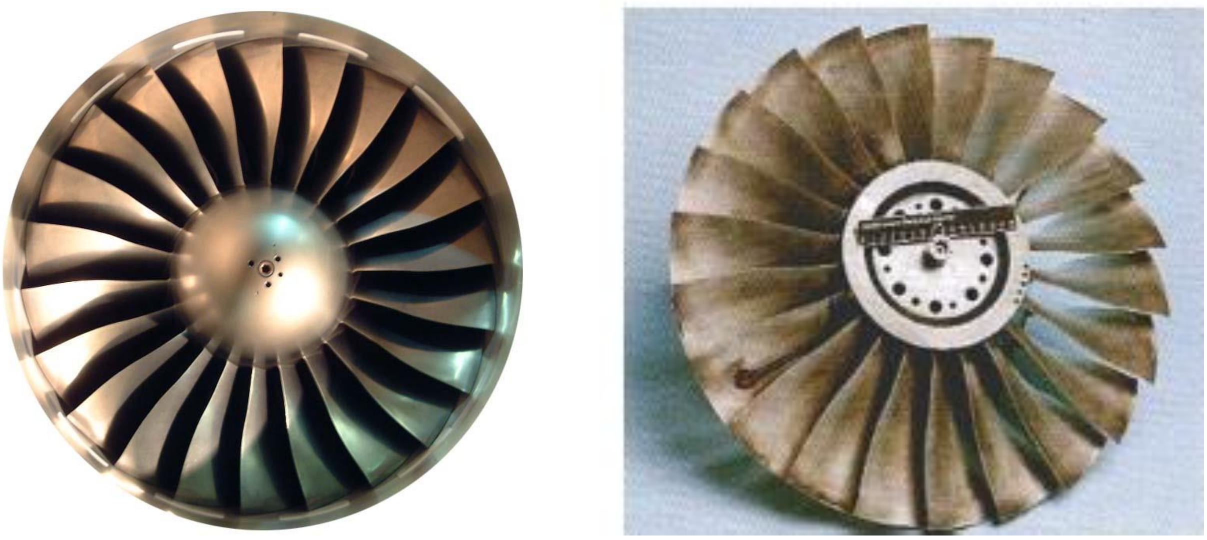

Figure 1: Front and perspective view of NASA Rotor 67 hardware

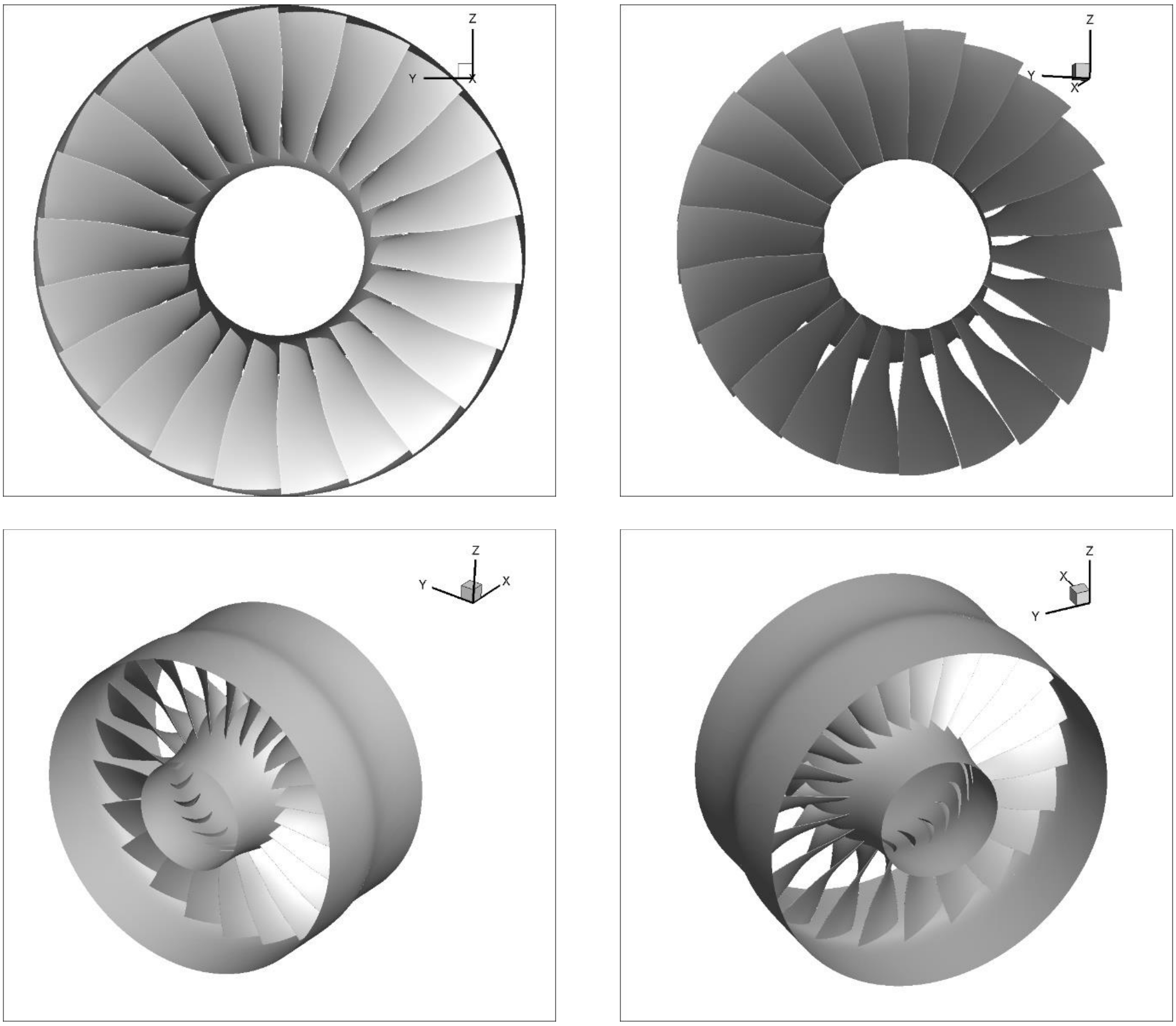

Figure 2: Solid model of NASA Rotor 67

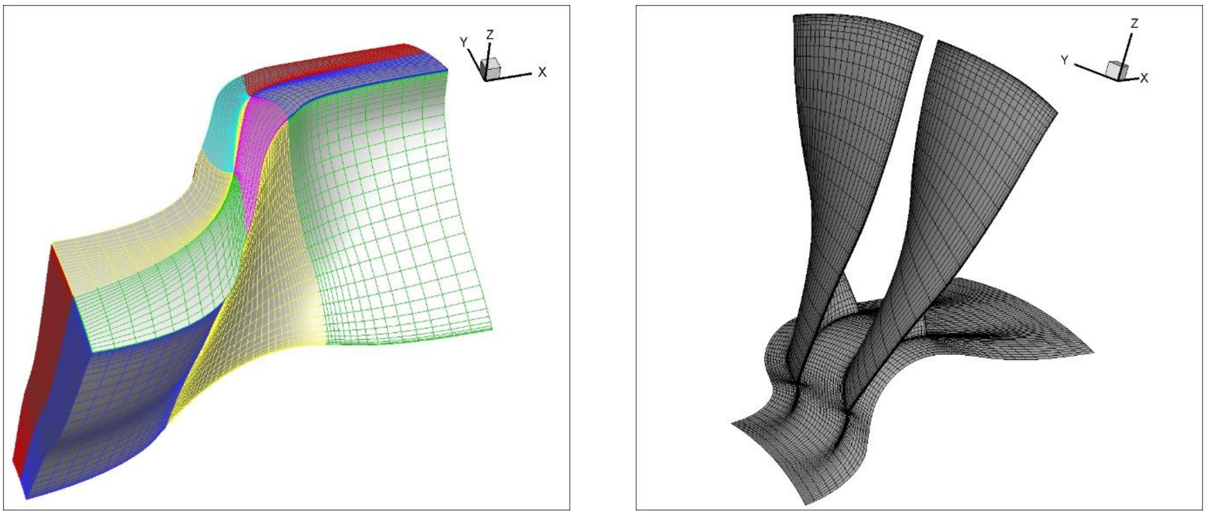

Figure 3: Multi block grid of flow domain and blade surface grid

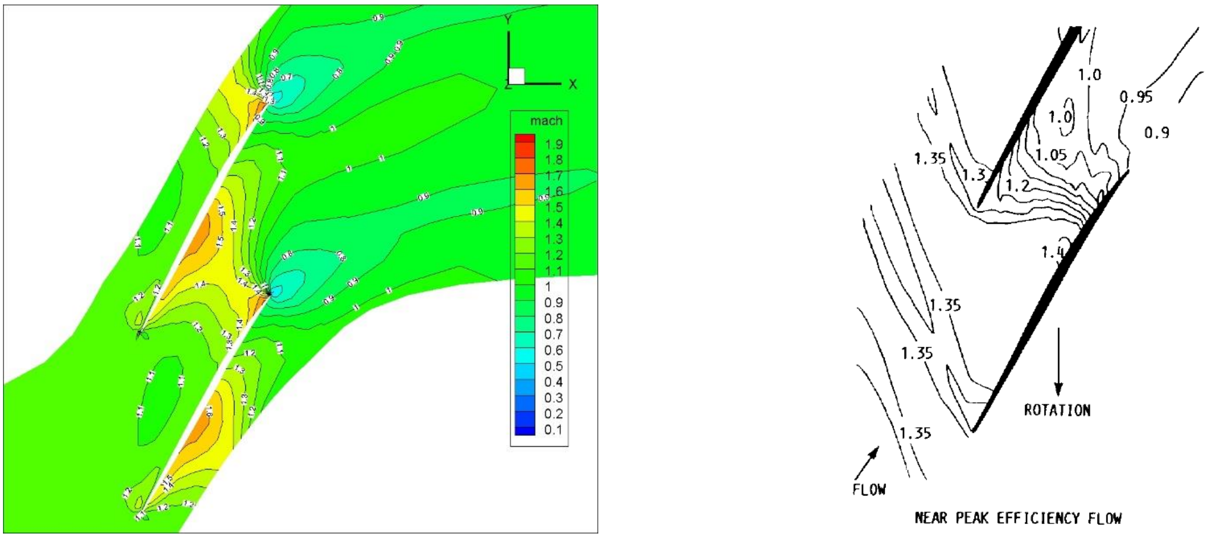


Figure 4.a: 10% span relative Mach number

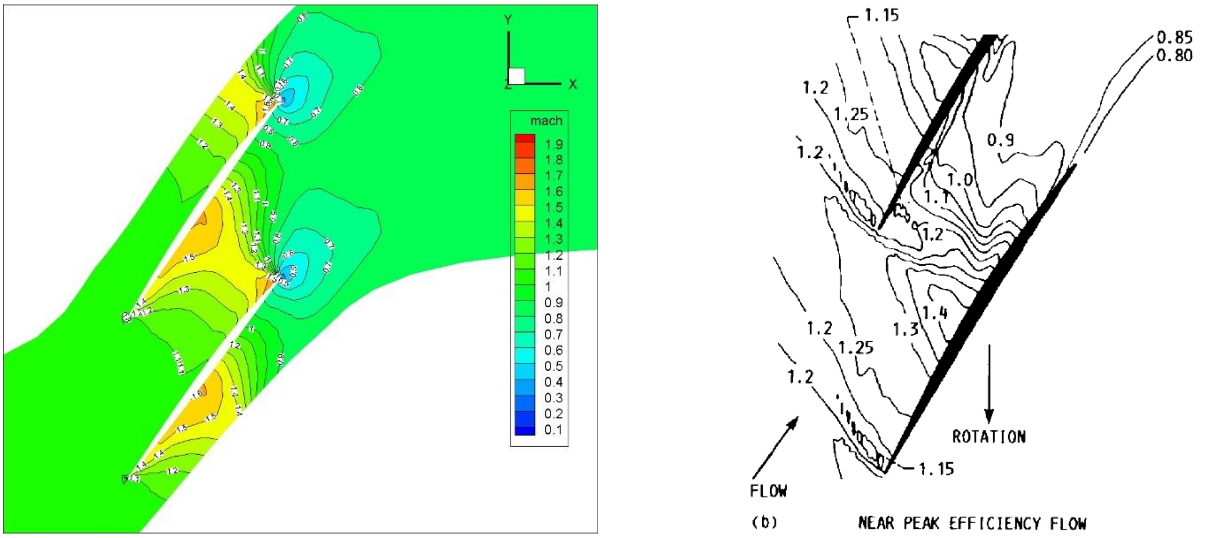


Figure 4.b: 30% span relative Mach number

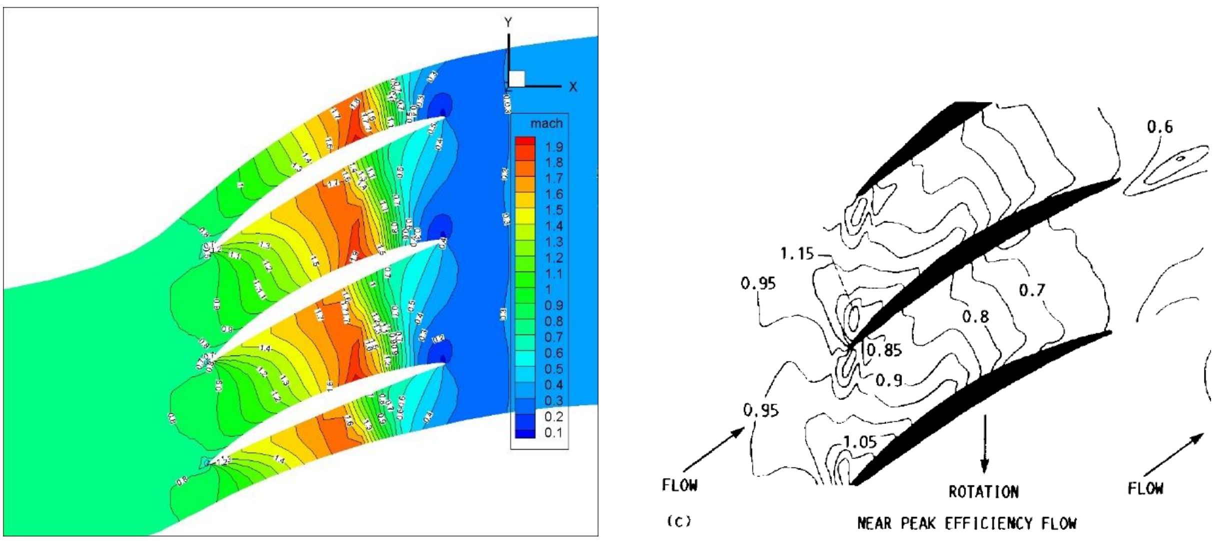


Figure 4.c: 70% span relative Mach number

Figure 4: Contours of relative Mach number near peak efficiency flow

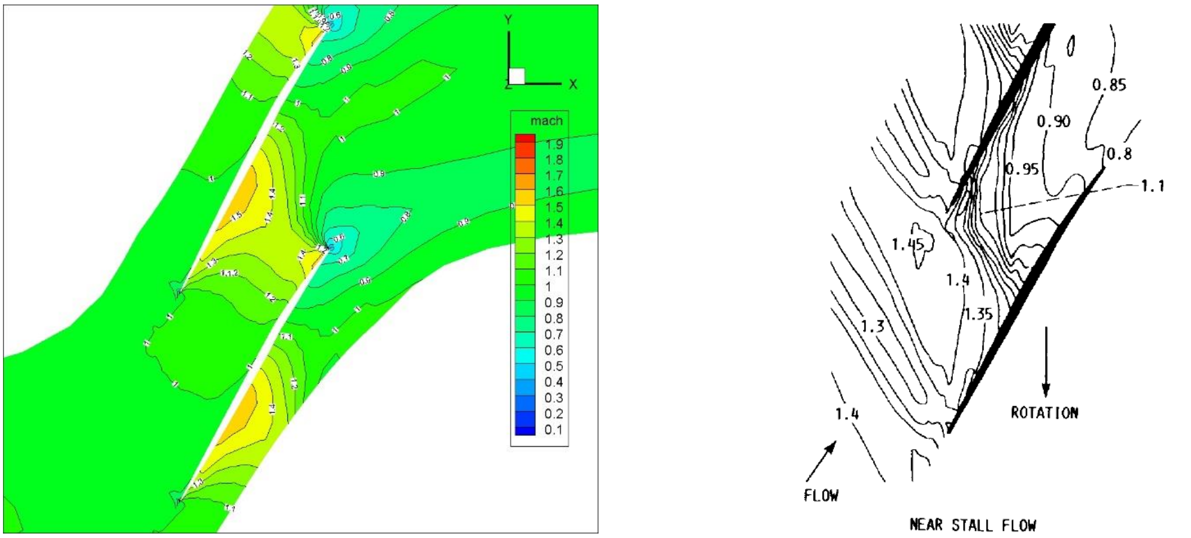


Figure 5.a: 10% span relative Mach number

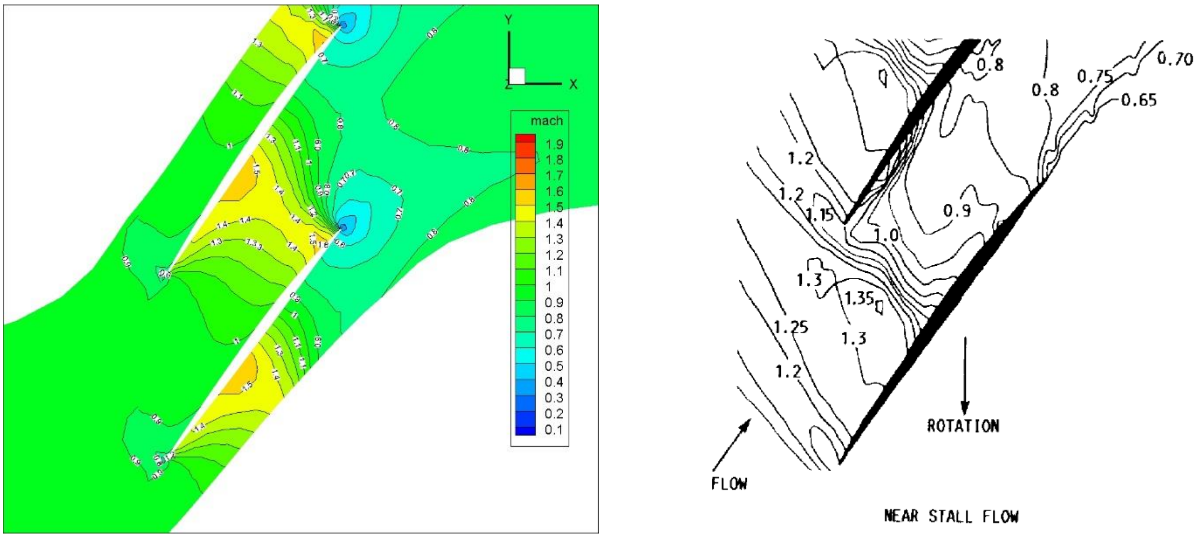


Figure 5.b: 30% span relative Mach number

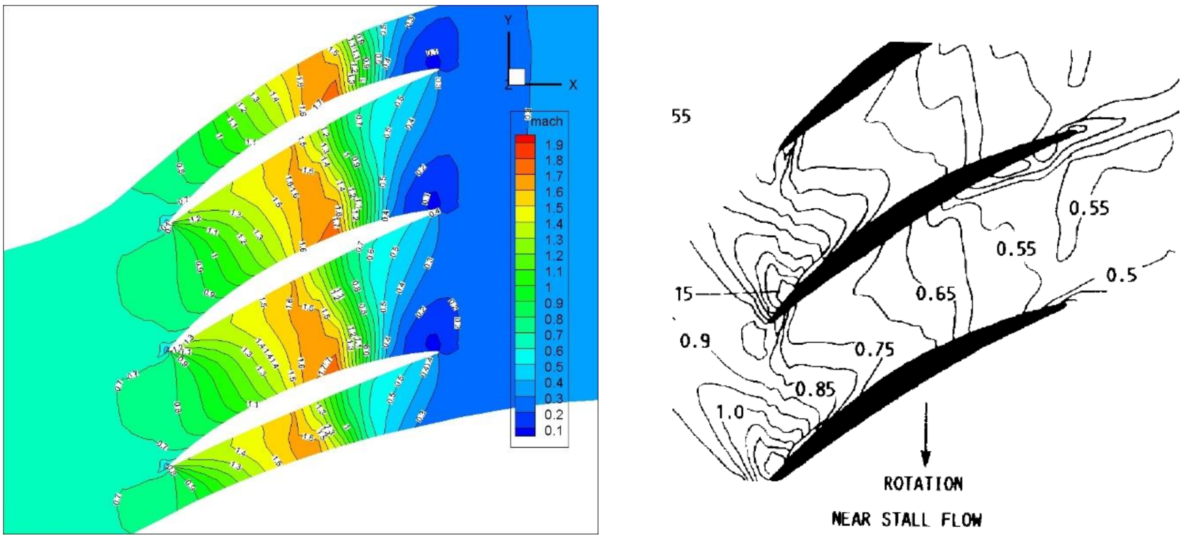


Figure 5.c: 70% span relative Mach number

Figure 5: Contours of relative Mach number near stall flow

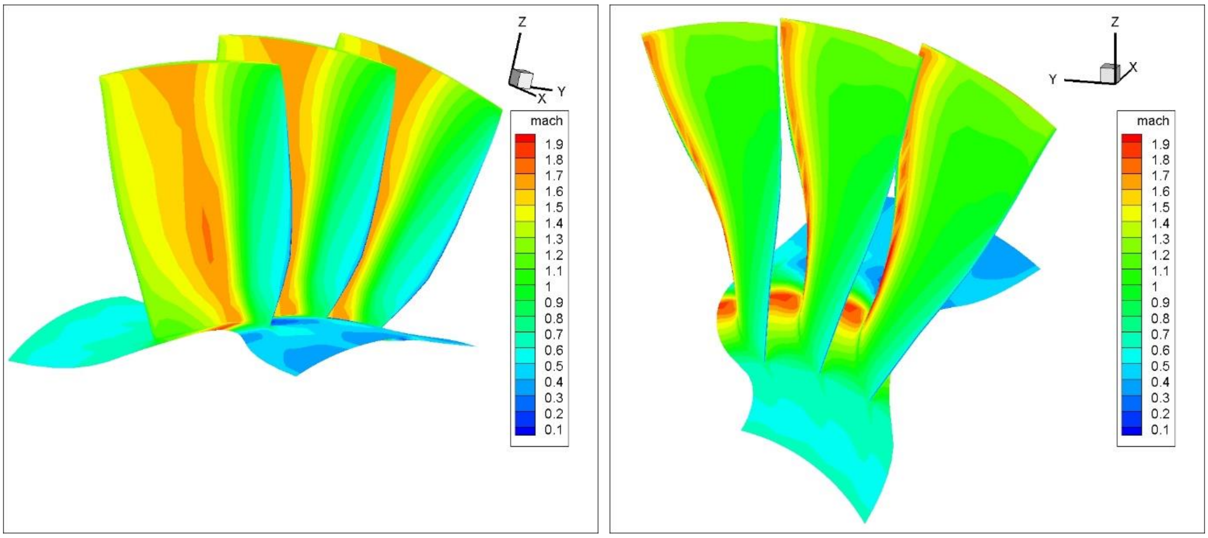


Figure 6: Relative Mach number on blade surfaces near peak efficiency flow

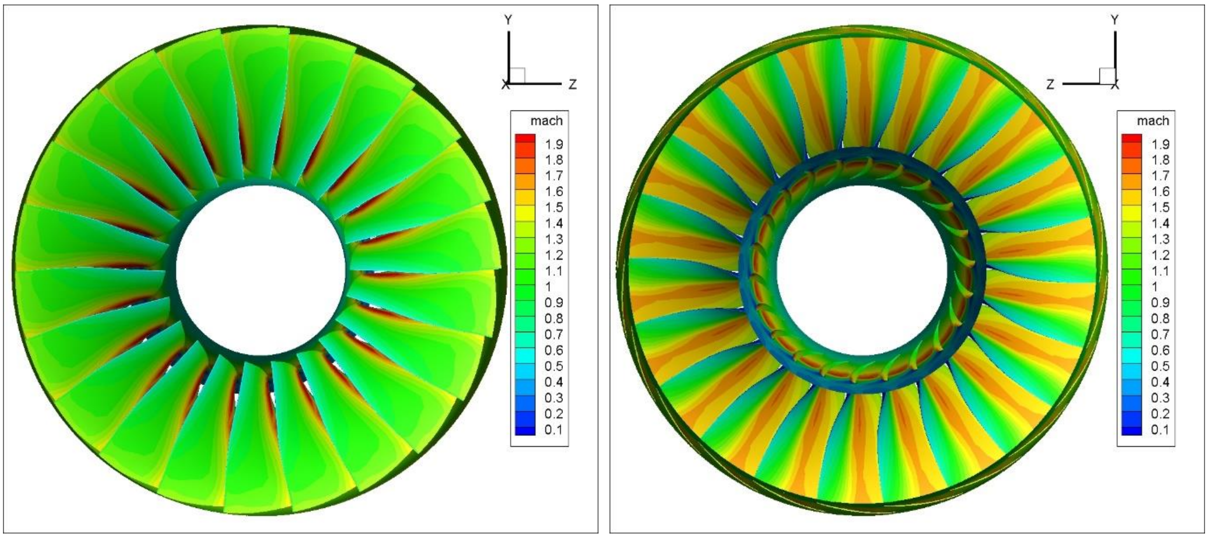


Figure 7: Relative Mach number at suction and pressure side near peak efficiency

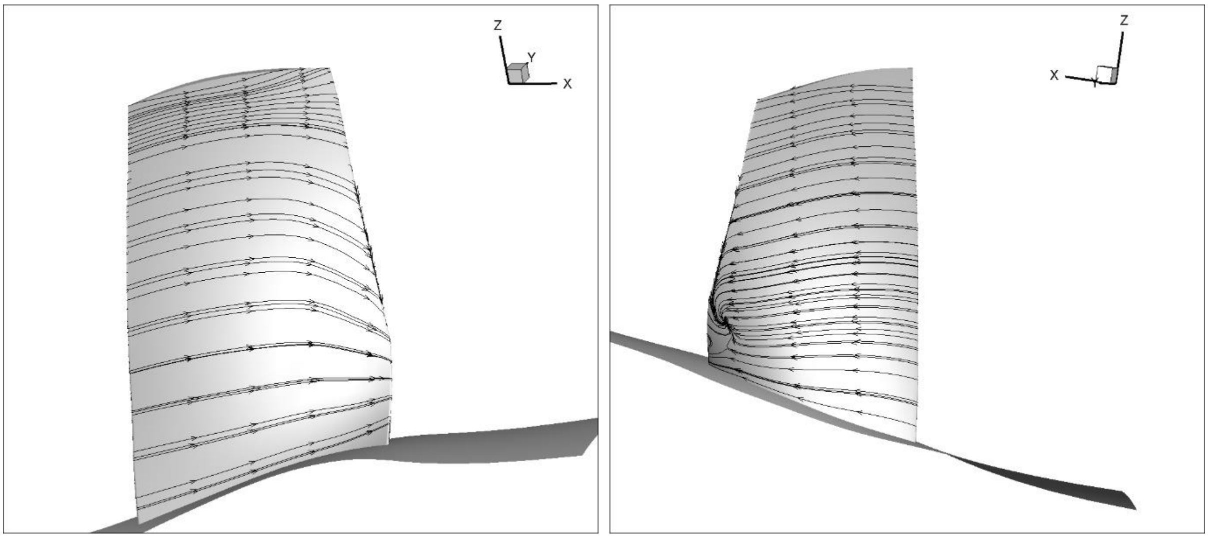


Figure 7: Stream traces near peak efficiency flow

## CONCLUSIONS

Test case is solved with 13 blocks which is obtained as optimum number of processor for parallel computing. Each block is solved by different processors in parallel computing. Speed up is reached to 3 as maximum value in 13 blocks/processors condition. Speed up is the rate of sequential computing time to parallel computing time. Increment of processor number is caused decrease in speed up due to communication cost of processes. MPI (Message Passing Interface) library is used as communicator. Point to point communication is used for sending and receiving the block interface boundary. Each process sends the residual by all to one communication command in MPI [Tokel and Yıldırım, 2016]. Grid is divided into blocks as possible as with equal cell numbers for load balance between processes. As a conclusion, multi block and parallel computing provides a significant computing efficiency in case of choosing optimum parameters.

Near peak efficiency flow corresponds with the 0.85 non-dimensional back pressure and near stall flow non-dimensional back pressure is 0.90. Both running conditions are compared with experimental results in three different span location. Especially in %10 and %30 span, flow profile and relative Mach number are similar to experimental results. Shock can be observed as delayed due to the Euler solution. As a result, shock wave is located to closer the trailing edge.

## References

Adamczyk, J.J. (1984) *Model Equation for Simulating Flows in Multistage Turbomachinery,* ASME Paper, No. 85-GT-226, November 1984.

Adamczyk, J.J., Celestina, M.L., Beach, T.A. and Barnett, M. (1990) *Simulation of Three Dimensional Viscous Flow Within a Multistage Turbine,* ASME Journal of Turbomchinery, Vol. 112, No. 3, p: 370-376, July 1990.

Agarwal, R.K. and Deese, J.E. (1987) *Euler Calculations for Flowfield of a Helicopter Rotor in Hover,* Journal of Aircraft, Vol. 24, No. 4, p: 231-238, April 1987.

Anderson, W.K., Thomas, J.L. and Leer, B.V. (1986) *Comparison of Finite Volume Flux Vector Splittings for the Euler Equations,* AIAA Journal, Vol. 24, No. 9, p: 1453-1460, September 1986.

Arnone, A. (1994) *Viscous Analysis of Three-Dimensional Rotor Flow Using a Multigrid Method,* ASME Journal of Turbomachinery, Vol. 116, No. 3, p: 435-445, July 1994.

Chen, J.P. (1991) *Unsteady Three-Dimensional Thin-Layer Navier-Stokes Solutions for Turbomachinery in Transonic Flow,* Ph.D. Dissertation, Mississippi State University, December 1991.

Chima, R.V. and Yokota, J.W. (1990) *Numerical Analysis of Three-Dimensional Viscous Internal Flows,* AIAA Journal, Vol. 28, No. 5, p: 798-808, May 1990.

Davis, T.A. (2003) *UMFPACK Version 4.1 User Manual,* University of Florida, 2003.

Ghosh, A.R. (1996) *Solutions to Three-Dimensional Thin-Layer Navier-Stokes Equations in Rotating Coordinate for Flow through Turbomachinery,* M.S. Thesis, Mississippi State University, December 1996.

Holmes, D.G. and Tong, S.S. (1985) *A Three-Dimensional Euler Solver for Turbomachinery Blade Rows,* Journal of Engineering for Gas Turbines and Power, Vol. 107, p: 258-264, April 1985.

Knoll, D.A. and Keyes, D.E. (2004) *Jacobian-Free Newton-Krylov Methods: A Survey of Approaches and Applications,* Journal of Computational Physics, Vol. 193, No. 2, p: 357-397, January 2004.

Leer, B.V. (1979) *Towards the Ultimate Conservative Difference Scheme. V. A Second Order Sequel to Godunov's Method,* Journal of Computational Physics, Vol. 32, No. 1, p: 101-136, July 1979.

Leer, B.V. (1982) *Flux Vector Splitting for the Euler Equations,* ICASE Report, p: 82-30, September 1982.

Onur, O. and Eyi, S. (2005) *Effects of the Jacobian Evaluation on Newton's Solution of the Euler Equations,* International Journal for Numerical Methods in Fluids, Vol. 49, No. 2, p: 211-231, June 2005.

Saad, Y. and Schultz, M.H. (1986) *GMRES: A Generalized Minimal Residual Method for Solving Nonsymmetric Linear Systems,* SIAM Journal, Vol. 7, No. 3, p: 856-869, July 1986.

Schenk, O. and Gartner, K. (2004) *Solving Unsymmetric Sparse Systems of Linear Equations with PARDISO,* Journal of Future Generation Computer Systems, Vol. 20, No. 3, p: 475-487, April 2004.

Srinivasan, G.R., Baeder, J.D., Obayashi, S. and McCroskey, W.J. (1992) *Flowfield of a Lifting Rotor in Hover: A Navier-Stokes Simulation,* AIAA Journal, Vol. 30, No. 10, p: 2371 2378, October 1992.

Strazisar, A.J., Wood, J.R., Hathaway, M.D. and Suder, K.L. (1989) *Laser Anemometer Measurement in a Transonic Axial-Flow Fan Rotor,* NASA Technical Paper 2879, November 1989.

Tokel, M. and Yıldırım, A. (2016) *Private Communication,* August 2016.

Weber, K.F., Thoe, D.W. and Delaney, R.A. (1989) *Analysis of Three-Dimensional Turbomachinery Flows on C-Type Grids Using an Implicit Euler Solver,* ASME Paper, No. 89-GT-85, June 1989.

Yıldırım, A. (2017) *Aerodynamic Design Optimization Using 3-Dimensional Euler Equation and Adjoint Method,* M.S. Thesis, Middle East Technical University, January 2017.